Fluorescence Lifetimes of Tyrosine Residues in Cytochrome *c″* as Local Probes to Study Protein Unfolding

Melinda Noronha,[†,‡] Raquel Santos,[†] Emanuele Paci,[§] Helena Santos,[‡] and António L. Maçanita*[,†]

Departamento de Química, Instituto Superior Técnico, Universidade Técnica de Lisboa, 1049-001 Lisboa, Portugal, Instituto de Tecnologia Química e Biológica, Universidade Nova de Lisboa, Rua da Quinta Grande 6, Apartado 127, 2780-156 Oeiras, Portugal, Department of Physics and Astronomy, University of Leeds, Leeds, U.K.

Received: July 1, 2008; Revised Manuscript Received: December 16, 2008

Time-resolved fluorescence spectroscopy was used to show that multiple tyrosine residues of a protein can serve as localized probes of structural changes during thermal unfolding. Cytochrome *c″* from *Methylophilus methylotrophus*, which has four tyrosine residues, was chosen as a model protein. The procedure involved, first, the assignment of the experimental decay times to the tyrosine residues, followed by the interpretation of the changes in the decay times and pre-exponential coefficients with temperature. We found that the fluorescence decays of cytochrome *c″* are double-exponential from 23 to 80 °C, with decay times much shorter than those of the parent compound *N*-acetyl-tyrosinamide; this quenching was ascribed to dipole−dipole energy transfer from the tyrosine residues to the heme. The tyrosine−heme distances (R) and theoretical decay times, τ_{comp}, were estimated for each tyrosine residue. The analysis of the simulated decay generated with τ_{comp}, showed that a double-exponential fit is sufficient to describe the four decay times with two pre-exponential coefficients close to values observed from the experimental decay. Therefore, the decay times at 23 °C could be assigned to the individual tyrosine residues as τ_1 to Tyr-10 and Tyr-23 (at 20.3 Å) and τ_2 to Tyr-12 and Tyr-115 (at 12−14 Å). On the basis of this assignment and MD simulations, the temperature dependence of the decay times and pre-exponential coefficients suggest that upon unfolding, Tyr-12 is displaced from the heme, with loss of the structure of α-helix I. Moreover, Tyr-115 remains close to the heme and the structure in this region of the protein is not altered significantly. Altogether the data support the view that the protein core, comprising the heme and the four α-helices II to V, is clearly more stable than the remaining region that includes α-helix I and the loop between residues 19−27.

Introduction

Time-resolved fluorescence spectroscopy (TRFS) can be successfully applied to follow protein structural changes during thermal and chemical unfolding. We have previously shown that proteins with single buried chromophores, such as bovine ubiquitin (UBQ), with a single tyrosine residue[1] and *Staphylococcus aureus* nuclease A (SNase A), with a single tryptophan,[2] display single-exponential fluorescence decays in the native state at pH 1.5 and 7, respectively. Upon unfolding, the decays become multiexponential because the lifetimes of tyrosine and tryptophan are sensitive to water exposure. The resulting separation of the contributions of native and unfolded protein in the fluorescence decay allowed the direct determination of mole fractions of the native and unfolded states and derivation of unfolding equilibrium constants as a function of temperature and denaturant concentration.

Fluorescence decays of multichromophoric proteins are in general multiexponential, even in the native state, not only because of the varying degree of multiple solvent-exposed chromophores but also due to the presence of photophysical processes such as proton,[1] electron,[3] or energy transfer,[4] involving the chromophores and nearby amino acids or prosthetic groups. Thus, when the chromophores are located in different regions within the protein, such that each microenvironment determines a sufficiently different decay time, the decay will be multiexponential. Each exponential term will refer to a given chromophore, allowing us to track changes that occur during unfolding in the structure of the protein regions where the chromophores are located.

In the case of ribonuclease A, a protein with six tyrosine residues, we have shown that the fluorescence decay times are controlled by long-range excited-state electron transfer from the tyrosine residues to disulfide bridges with a $\Delta G_{ET} \approx 0$ (3). As a result, the fluorescence decay times of each tyrosine residue are governed by their distance (R) to the nearest disulfide bridge. Among the six tyrosine residues, four were at the same distance of $R = 5.5$ Å and were all described by a single decay time of $\tau_1 \approx 30$ ps, one at $R = 6.9$ Å corresponding to a decay time of $\tau_2 \approx 200$ ps and the last at $R = 12.3$ Å described with $\tau_3 = 1.76$ ns. Hence, crucial to the assignment of decay times to individual tyrosine residues in cytochrome *c″* is the identification of the presence of possible quenching mechanisms.

In this paper, we explore the possibility of using this technique to study *Methylophilus methylotrophus* cytochrome *c″* (Cyt *c″*), a mono-heme protein with four tyrosine residues (Tyr-10, Tyr-12, Tyr-23, and Tyr-115) and no tryptophans. Cytochrome *c″*

* To whom correspondence should be addressed. E-mail: macanita@ist.utl.pt. Address: Departamento de Engenharia Quimica, Instituto Superior Tecnico, Av. Rovisco Pais s/n 1049-001 Lisboa, Portugal.
[†] Universidade Técnica de Lisboa.
[‡] Universidade Nova de Lisboa.
[§] University of Leeds.

10.1021/jp805781r CCC: $40.75
Published on Web 02/27/2009

CHART 1: 3-D Image of the Structure of Cytochrome *c″*[a]

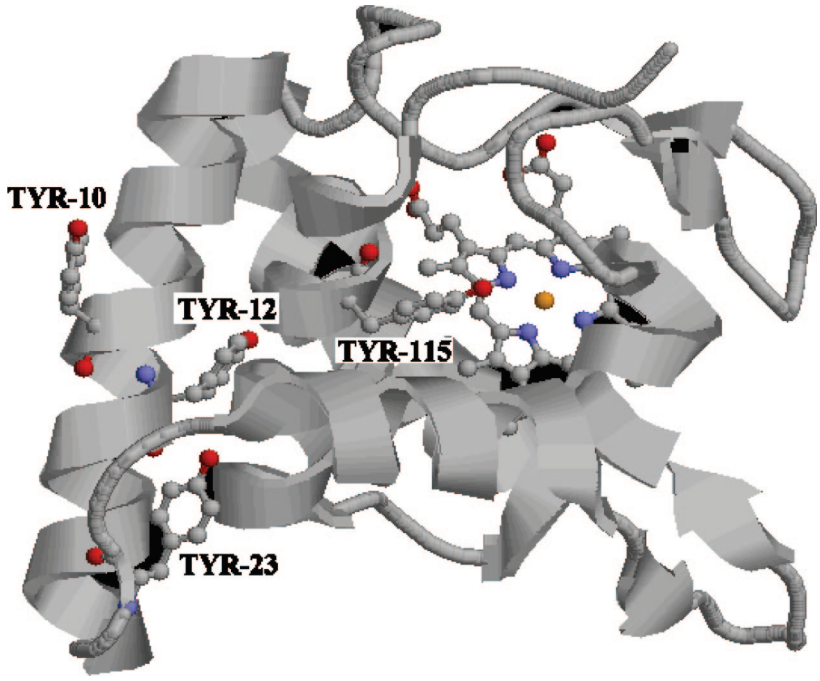

[a] Structure shows its single heme and four tyrosine residues, of which Tyr-10 and Tyr-12 are located on α helix-I, Tyr-23 on a loop between helices I and II, and Tyr-115 is located on the last helix V.

is a mono heme protein with 124 amino acids (14.2 kDa), whose physiological function remains unknown. The three-dimensional structure has been resolved by NMR spectroscopy (1E8E)[5] and by X-ray crystallography (1GU2) (Chart 1).[6] It has five α helices and four β strands.[6] Tyr-10 and Tyr-12 are located in the N-terminal region in helix I (Thr-3:Asn-20), Tyr-23 is on a loop between helix I and helix II (Thr-29:Asn-36), and Tyr-115 is located in the last helix V (Ser-107:Thr-118), which is close to the heme. The heme is covalently attached to the peptide backbone of the protein by two C−S bonds formed between the porphyrin ring and cysteine residues, Cys-49 and Cys-52. The iron of the heme is attached to two histidine ligands (His-53 and His-95) in the oxidized form. The structure is related to class I cytochromes with the additional helix I, and the axial histidinyl residues are found in an unusual perpendicular orientation.[5] It has one disulphide bridge (Cys-96−Cys-104), which is uncommon in *c*-type cytochromes, but essential to the detachment of the axial histidine (His-95).[6]

By comparing the fluorescence of hemoglobin and horseradish peroxidase before and after the removal of the heme, Weber and Teale were the first to demonstrate that the presence of the heme induces fluorescence quenching of tryptophan resultant of nonradiative electronic energy transfer.[7] During the last 20 years, there has been numerous papers reporting on the fluorescence of heme-proteins such as hemoglobin,[8] myoglobin,[9] and horseradish peroxidise.[10] Most of these studies were focused on the fluorescence quenching of tryptophan residues by the heme via resonance energy transfer, which is dependent on the distance (R) between the tryptophan residues and the heme. Here, we explore the quenching of tyrosine residues by the single heme of cytochrome *c″* to carry out the assignment of the fluorescence decay times to the individual tyrosine residues and then use the changes in the fluorescence decay times and pre-exponential coefficients during thermal unfolding to probe local changes in the protein structure.

Materials and Methods

Cytochrome *c″* was purified from *Methylophilus methylotrophus* as described elsewhere.[11] Recombinant cytochrome *c″* was expressed in BL21 (DE3) cells and purified as previously described.[12] Protein concentration utilized for absorption and fluorescence spectroscopy varied from 0.6 to 1.0 mg/ml and 0.22 to 0.6 mg/ml for DSC measurements.

UV-absorption and fluorescence spectra were measured using a Beckman Coulter DU 800 spectrophotometer and a SPEX Fluorog 212I spectrofluorimeter, respectively.

Time-resolved fluorescence (TRFS) measurements were carried out using the time-correlated single photon counting technique as previously described,[13] except for the electronic detection system (SPC-630 board module, from Becker & Hickl GmbH). The samples were excited with the vertically polarized frequency-tripled output of a mode-locked Ti-Sapphire LASER (Spectra Physics Tsunami), with a repetition rate of 82 MHz. Emission was collected at 90°, passed through a polarizer at 54.7° (Glen-Thompson), a monochromator (Jobin Yvon H20), and detected with a microchannel plate photomultiplier (MCP-PT Hamamatsu R3809u-50). The laser pulses were monitored with a fast photodiode (Becker & Hickl GmbH) and used as starts for the SPC-630. The instrumental response was in the 18−20 ps fwhm. Alternate collection of pulse and sample decays was performed, until about $5 \times 10^3-10^4$ detected counts at the maximum of the fluorescence signal. The fluorescence decays were deconvoluted on a PC, using George Striker's Sand program.[14] The fluorescence decays were measured from 23 to 80 °C at intervals of 2.5 and 5 °C using several fresh samples. This was necessary because exposure to high temperatures and UV irradiation, during the relatively long acquisition times of the decays, induced thermal and/or photodegradation of the protein.

Differential scanning calorimetry (DSC) measurements were carried out on a VP-DSC microcalorimeter from Microcal equipped with 0.51 mL cells and controlled by the VP-viewer

program. Calibration of temperature and heat flow was carried out according to the MicroCal instructions. The samples were extensively dialyzed (using a SpectraPor membrane with a molecular weight cutoff of 3500 Da) at 4 °C against the buffer and further degassed prior to the calorimetric experiments. The samples were heated from 10 to 100 °C at a scan rate of 1 °C/min and the calorimetric cells were kept under an excess pressure of 28 psi during the scan to avoid bubble formation during the experiments. Thermal unfolding of cytochrome *c″* was carried out in 10 and 50 mM phosphate buffer at pH 7.6. The thermograms were analyzed using the DSC support software provided by MicroCal, using as model a non-two state transition with ΔC_p.

CD spectra were recorded using the JASCO J-720 spectropolarimeter, equipped with Peltier temperature control. The protein concentration was 7 μM at pH 7.6 in 10 mM phosphate buffer and a cylindrical quartz cell with a 1-mm path length was used. Data were collected between 190 and 240 nm at 1-nm intervals with a dwell time of 1.5 s and each spectrum is an accumulation of 5 scans. A series of individual experiments were recorded at 25, 40, 61, 66, and 71 °C to monitor changes in ellipticity as a function of increasing temperature. The results are expressed in terms of mean residue ellipticity in deg cm^2 dmol^{-1}, according to $[\Theta]_{mrw,\lambda} = (\theta_\lambda) \times 100 \times M_r/lcn$ where M_r is the molecular weight of Cyt *c″* (14318.11 g/mol), θ is the observed ellipticity in degrees, l is the path length in cm, c is the protein concentration in g/l, and n is the number of residues (124 residues). The changes in the secondary structure were determined upon subtraction of the absorption of buffer and further analyses of the complete spectra in the region from 190 to 240 nm using the K2D2 software program. The best fits for both native (at 25 °C) and unfolded (at 71 °C) protein are presented in Supporting Information.

MD simulations were performed with the program CHARMM[15] using the all-atom force-field CHARMM22[16] and a generalized Born continuum model to include the effects of the solvent.[17] Starting from the NMR structure, 1E8E,[5] we first performed a short steepest descent minimization to remove possible steric clashes, followed by a slow heating to the desired temperatures, and then performed canonical simulations lasting between 2 and 4 ns. At 27 °C, the protein remains stable and the rmsd reaches a plateau at about 2 Å after 0.5 ns and never exceeds 2 Å during the whole duration of the simulation (4 ns). At higher temperatures, the TRFS data indicates residual structure. Therefore, MD simulations were carried out at temperatures of 127, 177, and 227 °C and the structure at 177 °C was chosen as the structure (rmsd ≈ 5 Å, showing regions with and without structure) that probably corresponds to the TRFS data at 80 °C. Simulation at higher temperatures would eventually lead to loss of all structure, which would not correspond to the experimental data. Langevin dynamics were used with a low friction coefficient (1 ps^{-1}) to accelerate the sampling relative to a water-like friction. The integration step was 2 fs for all of the simulations performed.

Results

Absorption and Fluorescence Spectra. The UV-absorption spectrum of oxidized Cyt *c″* in aqueous solution at pH 7.4, and that of the model compound *N*-acetyl-tyrosinamide (NAYA) in dioxane are shown in Figure 1. The spectrum of Cyt *c″* shows the absorption of the heme: the B bands at $\lambda = 406$ nm (corresponding to the Soret or γ band) and $\lambda = 349$ nm (corresponding to the ε band), and the Q bands (or α and β bands) centred at $\lambda = 521$ nm. In addition to these bands, the spectrum shows the absorption of the tyrosine residues with maximum at $\lambda_{abs} = 279$ nm, which matches the absorption maximum of the model compound *N*-acetyltyrosinamide NAYA (279 nm in dioxane).[13] The wavelength of maximum absorption of the tyrosine residues in Cyt *c″* is in agreement with the protein structure, that is, three tyrosine residues are buried and one is ~50% exposed.

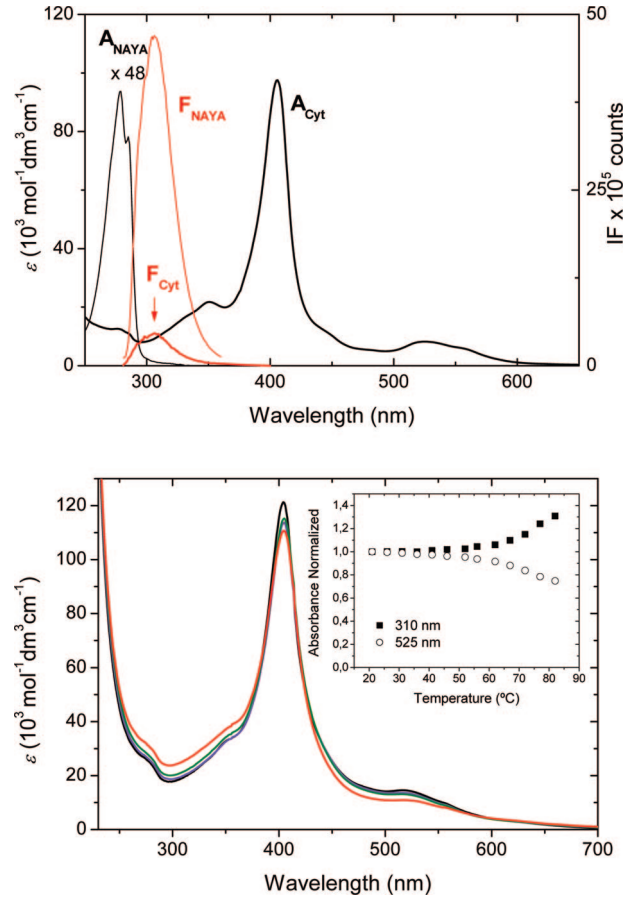

Figure 1. Absorption (black) and emission (red) spectra of oxidized (Cyt *c″*) at pH 7.4 in 25 mM Tris HCl: (a) The absorption spectrum shows the Soret band at $\lambda = 406$ nm and the maximum absorption of the tyrosine residues at $\lambda = 279$ nm, similar to the maximum absorption of parent compound, *N*-acetyltyrosinamide in dioxane (NAYA), which is amplified 48 times. The emission spectra of Cyt (F_{Cyt}) and NAYA (F_{NAYA}) show maximum emission at almost the same wavelength ($\lambda = 306$ nm) with a 10-fold decrease in the fluorescence intensity in the case of Cyt *c″*. (b) The absorption spectrum shows a 1-nm red-shift of the Soret band and a 8.7% reduction in the molar extinction coefficient from 20 °C (black) to 80 °C (red). The normalized absorbance curves (inset) show a gradual decrease at $\lambda = 525$ nm and a corresponding increase at $\lambda = 310$ nm above 35 °C.

Figure 1 also shows the fluorescence spectra of Cyt *c″* and NAYA upon excitation at $\lambda = 278$ nm. Both spectra show maximum emission at $\lambda = 306$ nm but the quantum yield of cytochrome *c″* ($\phi_F = 0.022 \pm 0.011$) is reduced ~10-fold with respect to the parent compound NAYA in dioxane ($\phi_F = 0.18 \pm 0.010$). The fluorescence of the tyrosine residues of Cyt *c″* overlaps with the absorption spectrum of Cyt *c″* heme (Figure 1).

As the temperature increases from 21 to 82 °C, the absorption spectra show a 1-nm red-shift and a 8.7% reduction in the molar extinction coefficient (ε) of the Soret band (Figure 1b). Interestingly, the spectra show a decrease in the ε at $\lambda = 525$ nm and an increase at $\lambda = 310$ nm above 35 °C up to 82 °C, which can not be attributed to the usual spectral broadening as the temperature increases (Figure 1b inset).

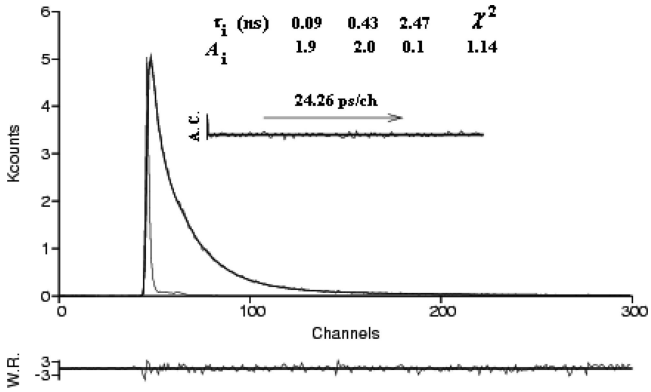

Figure 2. Fluorescence decay of cytochrome c'' at pH 7.4 in 25 mM TrisHCl with $\lambda_{exc} = 281$, $\lambda_{em} = 298$ nm at 23 °C. The decay times τ_i, the pre-exponential coefficients normalized to $\Sigma A_i = 4$, the value of χ^2, the autocorrelation function (A.C.), and the weighted residuals (W.R.) are also shown.

The fluorescence spectra of Cyt c'' show no significant shift in the maximum wavelength from 20 to 80 °C similar to the small red-shift observed with NAYA in dioxane ($\lambda^{20\ °C} = 304$ nm; $\lambda^{80\ °C} = 305$ nm) and water ($\lambda^{20\ °C} = 306$ nm; $\lambda^{80\ °C} = 307$ nm).[13] The quantum yield of Cyt c'' however only shows a small decrease from $\phi_F{}^{20\ °C} = 0.022$ to $\phi_F{}^{80\ °C} = 0.015$, whereas the quantum yield of NAYA decreases significantly with increasing temperature and solvent polarity from $\phi_F{}^{20\ °C} = 0.186$ to $\phi_F{}^{80\ °C} = 0.168$ in dioxane and from $\phi_F{}^{20\ °C} = 0.050$ to $\phi_F{}^{80\ °C} = 0.025$ in water. This indicates the persistence of fluorescence quenching of the tyrosine residues in Cyt c'' at higher temperatures.

Time Resolved Fluorescence. TRFS measurements of Cyt c'' in 25 mM TrisHCl buffer at pH 7.6 at room temperature were carried out with three pairs of excitation and emission wavelengths: $\lambda_{exc} = 275$, $\lambda_{em} = 320$ nm; $\lambda_{exc} = 281$, $\lambda_{em} = 298$ nm; and $\lambda_{exc} = 266$, $\lambda_{em} = 310$ nm. Figure 2 shows the fluorescence decay of Cyt c'' with $\lambda_{exc} = 281$, $\lambda_{em} = 298$ nm at 23 °C. The analysis showed that sums of three exponential terms are needed to fit the data, with decay times of $\tau_0 = 2.47$ ns, $\tau_1 = 430$ ps, $\tau_2 = 90$ ps and pre-exponential coefficients normalized to four $A_0 = 0.10$, $A_1 = 2.0$, and $A_2 = 1.9$. However, the pre-exponential A_0 associated to the long decay time (τ_0) is very small and varies from sample to sample and with the excitation and emission wavelength. It was, therefore, assigned to an impurity; that is, the fluorescence decay of Cyt c'' is in fact double-exponential.

TRFS measurements of Cyt c'' in 10 mM phosphate at pH 7.6 were carried out at higher temperatures with $\lambda_{exc} = 280$ nm and $\lambda_{em} = 297$ nm. The long decay time of Cyt c'' τ_1 is constant from 23 to 50 °C within the experimental error, then increases up to 560 ± 20 ps at 65 °C and decreases slightly to 500 ± 20 ps at 80 °C. From 70 to 80 °C, τ_1 approaches the lifetime trend of NAYA in water (Figure 3a). The shorter decay time τ_2 shows a similar profile, of an increase up to 88 ps at 65 °C and a slight decrease to 72 ± 10 ps at 80 °C. The overall variation is small, not much greater than the experimental error (Figure 3a).

From 23 to 55 °C, the pre-exponential coefficients are constant within experimental error. The pre-exponential A_1 associated to the long decay time τ_1 increases marginally from 2.0 at 23 °C to 2.25 at 65 °C and decreases again to 2.1 at 80 °C while A_2 shows the corresponding opposite trend of A_1 (Figure 3b).

Exposure to high temperatures and UV irradiation, during the relatively long acquisition times of the decays, induced thermal and/or photodegradation of the protein. This was

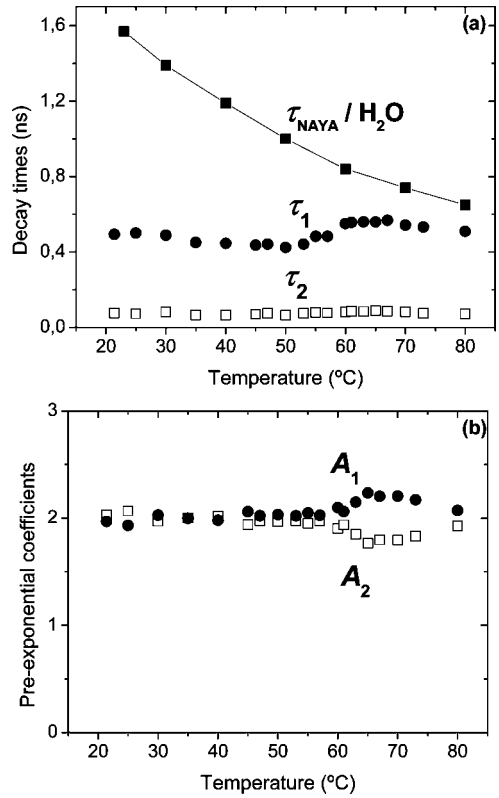

Figure 3. (a) The longer decay time of cytochrome c'' τ_1 (closed circles) is constant from 23 to 55 °C and increases from 460 ± 30 to 560 ± 20 ps at 65 °C and decreases to 500 ± 20 ps at 80 °C while τ_2 (open squares) shows a similar profile, of an increase up to 88 ps at 65 °C and a slight decrease to 72 ± 10 ps at 80 °C. Above 70 °C, the values of τ_1 approach the decay times of NAYA in neat water (closed squares). (b) The normalized pre-exponential coefficient A_1 (closed circles) is constant from 23 to 55 °C and increases marginally from 2.0 at 23 °C to 2.25 at 65 °C while A_2 (open squares) shows the corresponding opposite trend of A_1 (Figure 3b).

reflected by a ca. 10% decrease in the optical density (OD) of the absorption band of the tyrosines at $\lambda = 279$ nm and the appearance of new broad emission bands at ca. 390 and 430 nm after cooling the heated sample. The fluorescence decays also indicate protein degradation by an increase in the pre-exponential coefficient of the long decay time attributed to the impurity. However, the two other decay times and their pre-exponential coefficients were not altered. Thus, the fluorescence signal of the degradation product could still be isolated from that of the protein.

Differential Scanning Calorimetry (DSC) and Circular Dichroism (CD). DSC thermograms carried out in 10 mM phosphate buffer at pH 7.6 show a single transition with a $T_m = 61.9 \pm 1$ °C. DSC thermograms were also carried out in the same buffer conditions for two different protein concentrations of 0.4 and 0.6 mg/ml. The results showed similar values for T_m, ΔH^{cal} and ΔH^{VH} indicating that at least up to $T = T_m$, there is no indication of aggregation. However, at temperatures higher than the T_m, the protein degradation is evident from the progressively lower values of ΔH^{cal} with respect to ΔH^{VH} upon a successive second heating scan. However, the T_m and ΔH^{VH} remain the same.

CD spectra of Cyt c'' in 10 mM phosphate buffer, pH 7.6 at 25 °C (native state), 61 °C (close to T_m) and 71 °C (unfolded state) are shown in Figure 4. The spectrum at 25 °C shows the characteristic negative signals of the α-helix and β-sheet in the 200−240 nm region and the positive signal of the α-helix below

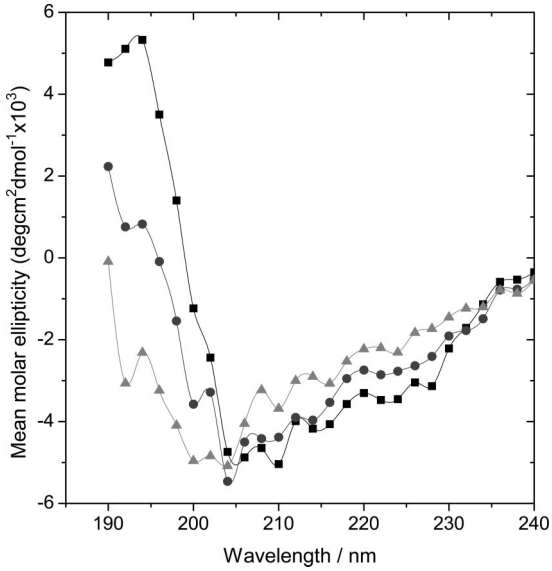

Figure 4. CD spectra of cytochrome *c″* at pH 7.6 in 10 mM phosphate at 25.0 °C (squares), 61.0 °C (circles), and at 71.0 °C (triangles) shows the prevalence of secondary structure even at 71 °C.

200 nm. At 71 °C the spectrum shows a strong decrease of the α-helix signal at ca. 195 nm due to the contribution of the negative signal of random coils below 210 nm. The spectrum also shows a significant persistence of α-helix and/or *β*-sheet structure in the unfolded state.

Analysis of the spectra using the software program K2D2, predicts a reduction from 14% α-helix and 34% *β*-sheet structure for the native protein at 25 °C to 6.9% α-helix and 29.3% *β*-sheet structure at 71 °C, indicating the presence of structure even at high temperature and above the T_m (Supporting Information, Figure SI.1).

Discussion

Assignment of Fluorescence Decay Times to Tyrosine Residues. On the basis of its structure and water exposure of its four tyrosine residues, the fluorescence decay of Cyt *c″* is expected to be double-exponential with lifetimes of $\tau_1 = 4.7$ and $\tau_2 = 3.7$ ns with pre-exponential coefficients normalized to four tyrosine residues equal to $A_1 = 3$ and $A_2 = 1$ corresponding to three buried tyrosine residues (solvent accessibility of less than 15%) and one tyrosine residue which is ∼50% exposed to water.[13] Thus, the presence of two much shorter decay times of $\tau_1 = 460 \pm 30$ and $\tau_2 = 80 \pm 20$ ps indicate the presence of a more efficient fluorescence quenching mechanism which determines the decay times other than solvent-accentuated excited-state electron transfer to the peptide backbone of the protein.[13] The protein structure shows that two of the tyrosine residues (Tyr-12 and Tyr-115) are at ca. 12−14 Å from the heme and the other two (Tyr-10 and Tyr-23) are at 20.3 Å. On the basis of the appreciable overlap of the tyrosine fluorescence with the heme absorption, they are probably quenched by resonance energy transfer to the heme. Hence, the shortest decay time is likely due to Tyr-12 and Tyr-115 and the longest to Tyr-10 and Tyr-23.

Quenching by Resonance Energy Transfer. The fluorescence decay time of a tyrosine residue in the presence of resonance energy transfer (τ_i) depends on its fluorescence lifetime in the absence of quenching (τ_0), the rate of energy transfer k_{EN}, and the rate of other possible quenching mechanisms such as electron/proton transfer (k_q) as given in eq 1

$$\tau_i = \frac{1}{\frac{1}{\tau_0} + k_{EN} + k_q} \quad (1)$$

At donor−acceptor distances substantially larger than the van der Waals distance, k_{EN} is given by eq 2, where R_0 is the Förster radius and R represents the donor−acceptor distance, in this case the tyrosine−heme center-to-center distance.

$$k_{EN} = \frac{1}{\tau_0}\left(\frac{R_0}{R}\right)^6 \quad (2)$$

According to eq 2, Tyr-12 and Tyr-115 should be strongly and similarly quenched and the other two (Tyr-10 and Tyr-23) less quenched.

The Förster radius R_0 is a constant for a given donor−acceptor pair and can be calculated using eq 3,

$$R_0 = 0.2108[\kappa^2 \phi_D n^{-4} \int_0^\infty I_D(\lambda)\varepsilon_A(\lambda)\lambda^4 d\lambda]^{\frac{1}{6}} \quad (3)$$

where κ^2 is the orientation factor (eq 4), ϕ_D is the fluorescence quantum yield of the donor (tyrosine) in the absence of resonance energy transfer, n is the refractive index of the medium in the wavelength range where the spectral overlap is significant, $I_D(\lambda)$ is the normalized fluorescence spectrum of the donor ($\int_0^\infty I_D(\lambda)d\lambda = 1$), λ is the wavelength in nm and $\varepsilon_A(\lambda)$ is the molar extinction coefficient of the acceptor.[18]

Among the variables that determine the R_0 value, n and κ^2 have a greater level of uncertainty associated to them. Energy transfer within a protein occurs in a microheterogeneous medium whose refractive index can not be measured with traditional methods. For example, for amino acids buried in the interior of a protein, the physical properties (e.g., polarizability) of the microenvironment are expected to be related to an organic solvent, while for amino acids on the surface the refractive index of water would better represent the microenvironment of these amino acids. Therefore, we expect values of the refractive index within a protein, to vary between 1.33 (for water at 23 °C) and 1.6 (for highly polarizable organic solvents). In the absence of a method to directly determine the refractive index of the medium in between each tyrosine residue and the heme, we have assumed a value of 1.4 for Tyr-10 (50% water exposed) and 1.6 for the remaining three tyrosine residues (buried in the protein). The variation from 1.33 to 1.6 can lead to an error of a factor of $(1.6/1.33)^{4/6} = 1.13$ in the determination of R_0, and a factor of 2 in the determination of k_{EN}.

The semirigid 3D structure of the protein also leads to difficulties in the determination of the orientation factor κ^2. There are three situations in which the value of κ^2 can be estimated with some confidence: If the donor and acceptor are able to freely rotate then we can assume a value of $\kappa^2 = 2/3$, if the donor and acceptor are in a rigid system where a single conformation exists then κ^2 can be accurately calculated, or if they are in a rigid system where all the possible conformations have the same probability, in which case a value of $\kappa^2 = 0.476$ could be assumed. However, in the case of tyrosine in proteins, none of the three conditions mentioned above are totally satisfied. An estimate of the values for κ^2 for each tyrosine can be obtained using eq 4

$$\kappa^2 = [(\bar{M}_D \cdot \bar{M}_A) - 3(M_D \cdot \bar{r})(\bar{M}_A \cdot \bar{r})]^2 = [\cos\theta_{DA} - 3\cos\theta_D \cos\theta_A]^2 \quad (4)$$

where $\bar{M}_D$ and $\bar{M}_A$ are the transition dipole moments of the donor and the acceptor respectively, $\bar{r}$ is the vector that joins the center of $\bar{M}_D$ and $\bar{M}_A$, θ_{DA} is the angle between $\bar{M}_D$ and $\bar{M}_A$, θ_D is the angle between $\bar{M}_D$ and $\bar{r}$, and θ_A is the angle between $\bar{M}_A$ and $\bar{r}$.

The calculation of κ^2 depends on the correct determination of $\bar{M}_D$ and $\bar{M}_A$. To some extent, progress has been made in the determination of the transition dipole moments. In the case of tyrosine, the transition dipole moment can be calculated using AM1 semiempirical method, which predicts the transition dipole along the long axis that unites C_1,C_4 of the phenyl ring and the oxygen atom of the hydroxyl group; that is, the transition dipole is along the ^1L_a axis.

The transition dipole of the heme is more complicated to determine. Attempts by Gryczynski et al. for hemeoglobin and myoglobin[4] using linear dichroism were made using model systems of metalloporphyrins in stretched polyvinyl alcohol films,[19] which have indicated the transition dipole to be in the plane of the porphyrin ring at an angle of 50−60° relative to the α-γ-meso axis of the porphyrin ring.

Values for κ^2 were calculated for each of the tyrosine residues of Cyt c'' in each of the 20 NMR structures. The spectral overlap integral was calculated using a value of $\varepsilon_A = 102375$ mol^{-1}dm^3 cm^{-1} and a value of the quantum yield (ϕ_F) for each tyrosine residue was used based on their respective solvent exposure and using previously determined values of quantum yield for NAYA in mixtures of dioxane/water.[13] Using the parametrization of these values, we calculated the R_0 values (R_{0teo}) for each tyrosine residue using eq 3. Average values of κ^2 and R_{0teo} are presented in Table 1.

We then calculated the rate of quenching by resonance energy transfer k_{EN} and the computed fluorescence decay times of each tyrosine residue (τ_{comp}) (Table 1) using R values calculated from the MD simulation at 27 °C and the fluorescence lifetime in the absence of quenching (τ_0). Taking into account the inherent errors associated to the determination of the correct refractive index within a protein (n), the orientation factor (κ^2), the quantum yield (ϕ_F) of each tyrosine residue, and the molar extinction coefficient of the acceptor (ε), the magnitude of the computed decay times is in reasonable agreement with the experimental decay times. However, four different decay times are predicted: 678, 628, 85, and 47 ps (Table 1).

Using the values of the four theoretical decay times, the corresponding tetra-exponential fluorescence decay was computed by convoluting the tetra-exponential function with an experimental pulse, and adding random Poissonian noise. The simulated decays were analyzed with sums of two, three, and four exponentials. The analysis showed that a double-exponential fit (Figure 5) is sufficient to describe the four decay times with $\tau_1 = 650$ and $\tau_2 = 70$ ps and pre-exponential coefficients ($A_1 = 2.05$ and $A_2 = 1.95$) close to values observed from the experimental decay ($\tau_1 = 460 \pm 30$ ps, $\tau_2 = 80 \pm 20$ ps; $A_1 = 2.05 \pm 0.05$, $A_2 = 1.95 \pm 0.05$). It is thus clear that the fluorescence decay times of the two more strongly quenched tyrosine residues (Tyr-12 and Tyr-115) are not well resolved experimentally and mixing of the two individual decay times results in an average decay time of 80 ± 20 ps. The longer theoretical decay time is greater than the observed $\tau_1 = 460 \pm 30$ ps, although small variations in n, κ^2, or ϕ_F could easily justify this difference. In fact, if we use values of κ^2 for Tyr-10, Tyr-12, Tyr-23, and Tyr-115 of 0.7, 0.5, 1.05, and 0.3, respectively, instead of those obtained from the NMR structures, the simulated fluorescence decay gives the same decay times and pre-exponential coefficients as experimentally observed. Hence, we assign Tyr-10 and Tyr-23 to τ_1 and Tyr-12 and Tyr-115 to τ_2 in native Cyt c''.

Thermal Unfolding. The profile of the fluorescence decay times of the tyrosine residues of Cyt c'' with increasing temperature, provides the following information on the structural changes of the protein upon thermal unfolding: (1) the persistence of a quenched decay time of $\tau_2 \approx 100$ ps from 23 to 80 °C indicates that either Tyr-12 or Tyr-115 remains close to the heme even at high temperatures, suggesting the presence of secondary structure even at 80 °C in the region where either Tyr-12 or Tyr-115 is located and (2) the increase in the decay time τ_1 from 55 to 70 °C indicates loss of some secondary structure. These indications are consistent with the information, resulting from the CD spectrum at the highest temperature (Figure 4), that secondary structure persists in the unfolded state of Cyt c''.

The fluorescence lifetime of NAYA in water τ_0 tends to decrease with increasing temperature as observed in Figure 3. Therefore, the increase in τ_1 is only possible if the individual distance R of one of the tyrosine residues also increases. As the heme is covalently attached to Cys-49 and Cys-52 in Cyt c'', and the detachment of the heme from the protein is not possible even at high temperatures; any change in R is only expected to result from changes in the secondary structure.

We carried out MD simulations at a number of temperatures at 127, 177, and 227 °C, which on the time scale of the simulations reached a rmsd value from the native structure of 3, 5, and 8 Å, respectively, thus providing a range of increasingly unfolded ensembles of structures. For a rmsd value = 5 Å at 177 °C, the protein shows regions with and without structure, possibly indicating the structure of Cyt c'' at 80 °C. This temperature (177 °C) was, therefore, chosen to calculate the tyrosine-heme distances at higher temperatures with the intent to explain the profile obtained by TRFS data at 80 °C.

From the MD simulation at 177 °C (Figure 6), we observe that essentially only one tyrosine residue Tyr-12 increases its distance from the heme, from $R = 14.2$ Å at 27 °C to $R = 24.6$ Å at 177 °C. If we assume that the simulation of Cyt c'' at 177 °C represents the unfolded protein at 80 °C, then using the values described in Table 2, decay time values of 430 ps (Tyr-10), 825 ps (Tyr-12), 284 ps (Tyr-23), and 32 ps (Tyr-115) were calculated on the basis of the Tyr distance from the heme (R) and solvent exposure obtained from the simulation at 177 °C. The analysis of the theoretical decay showed that a triple-exponential fit with decay times $\tau_1 = 860$ ps, $\tau_2 = 370$ ps, and $\tau_3 = 40$ ps and pre-exponential coefficients $A_1 = 0.93$, $A_2 = 2.10$, and $A_3 = 0.97$ is required (Figure 7a) and that this deviates from the experimentally observed double exponential decay at 80 °C ($\tau_1 = 510$ ps ($A_1 = 2.07$) and $\tau_2 = 72$ ps ($A_1 = 1.93$)). The MD simulation at 177 °C predicts a completely labile Tyr-12 ($R = 24.6$ Å) in a region with no residual structure, a solvent accessibility of 60%, a value expected for a tyrosine residue in a structured region of the protein. Hence, the MD simulations seem to be underestimating the solvent accessibility of residues in the denatured state. It would be more plausible to expect that an amino acid that is in a nonstructured region to be described by a solvent accessibility close to water while those in regions with structure to be described with a solvent accessibility less than 50%.

TABLE 1[a]

Tyr number	R (Å)	τ_0 (ns)	τ_i (ns)	ϕ_F	κ^2	SI[b] × 10^{13}	n	R_{0teo} (Å)	k_{EN} (ns^{-1})	k_{ET} (ns^{-1})	τ_{comp} (ns)
10	20.3	3.10	0.440	0.116	0.40	17.6	1.4	25.1	1.15		0.677
12	14.2	4.45	0.087	0.167	0.68	17.6	1.6	26.6	9.80	1.7	0.085
23	20.3	4.56	0.440	0.171	0.70	17.6	1.6	26.9	1.37		0.628
115	11.7	4.86	0.087	0.182	0.46	17.6	1.6	25.3	21.19		0.047

[a] Comparison of the experimental decay times (τ_i) at 23 °C and the computed decay times (τ_{comp}) calculated using equation 1−3 and the fluorescence lifetimes (τ_0) of each tyrosine (Tyr) residue based on their solvent exposure, the distance (R) of each tyrosine residue to the iron (Fe^{3+}) of the heme, the rate of energy transfer (k_{EN}), the rate of electron transfer to the nearest disulfide bridge (k_{ET}), and the characteristic Förster radius (R_{0teo}) estimated using eq 3, the quantum yield (ϕ_F) of each tyrosine residue, the orientation factor (κ^2), spectral integral (SI), and refractive index (n). [b] In M^{-1} cm^{-1} nm^4.

TABLE 2[a]

Tyr number	R (Å)	τ_0 (ns)	ϕ_F	κ^2	SI[b] × 10^{13}	n	R_{0teo} (Å)	k_{EN} (ns^{-1})	k_{ET} (ns^{-1})	τ_{comp} (ns)
10	20.3	2.54	0.095	0.67	17.6	1.4	26.4	1.93	-	0.430
12	24.6	1.66	0.040	0.67	17.6	1.4	24.6	0.61	-	0.825
23	17.8	3.41	0.127	0.67	17.6	1.5	26.5	3.22	-	0.284
115	11.7	4.0	0.149	0.67	17.6	1.6	26.1	30.86	-	0.032

[a] The computed decay times (τ_{comp}) at 80 °C calculated using eq 1−3 and the fluorescence lifetimes (τ_0) of each tyrosine (Tyr) residue based on their solvent exposure and the distance (R) of each tyrosine residue to the iron (Fe^{3+}) of the heme calculated from MD simulations at 177 °C, the rate of energy transfer (k_{EN}), the rate of electron transfer to the nearest disulfide bridge (k_{ET}), and the characteristic Förster radius (R_{0teo}) estimated using eq 3, the quantum yield (ϕ_F) of each tyrosine residue, the orientation factor (κ^2), spectral integral (SI), and refractive index (n). [b] In M^{-1} cm^{-1} nm^4.

TABLE 3[a]

Tyr number	R (Å)	τ_0 (ns)	ϕ_F	κ^2	SI[b] × 10^{13}	n	R_{0teo} (Å)	k_{EN} (ns^{-1})	k_{ET} (ns^{-1})	τ_{comp} (ns)
10	20.3	2.54	0.095	0.67	17.6	1.40	26.4	1.93	-	0.430
12	24.6	0.65	0.024	0.67	17.6	1.33	21.8	0.75	-	0.437
23	17.8	0.65	0.024	0.67	17.6	1.33	28.7	5.21	-	0.148
115	11.7	4.0	0.149	0.67	17.6	1.60	26.1	30.86	-	0.032

[a] The computed decay times (τ_{comp}) at 80 °C calculated using eq 1−3 and the fluorescence lifetimes (τ_0) of each tyrosine (Tyr) residue based on their solvent exposure, the distance (R) of each tyrosine residue to the iron (Fe^{3+}) of the heme, the rate of energy transfer (k_{EN}), the rate of electron transfer to the nearest disulfide bridge (k_{ET}), and the characteristic Förster radius (R_{0teo}) estimated using eq 3, the quantum yield (ϕ_F) of each tyrosine residue, the orientation factor (κ^2), spectral integral (SI), and refractive index (n). [b] In M^{-1} cm^{-1} nm^4.

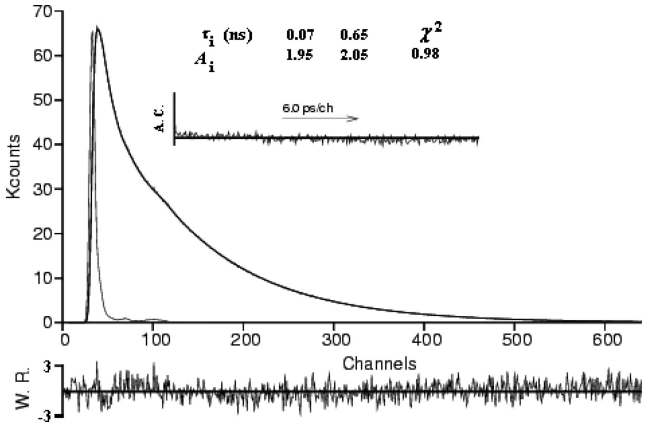

Figure 5. Analysis of a theoretical fluorescence decay of cytochrome c'' with 75000 counts at the maximum was generated using the four decay times presented in Table 1, with noise. The decay can be fitted with a double-exponential with decay times and pre-exponentials of τ_1 = 650 ps (A_1 = 2.05) and τ_2 =70 ps (A_2 = 1.95).

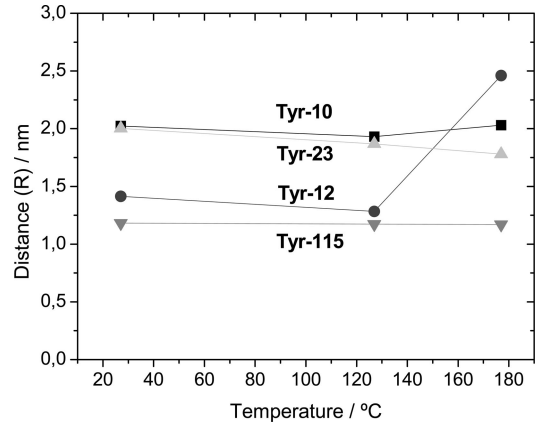

Figure 6. Distance (R) of each tyrosine residue to the haem, Tyr-10 (squares), Tyr-12 (circles), Tyr-23 (up triangles), and Tyr-115 (down triangles) calculated from MD simulations at 27, 127, and 177 °C shows essentially a change in the distance of Tyr-12 at higher temperatures.

If ϕ_D or n are slightly different from the values presented in Table 2, such that Tyr-12 and Tyr-23 are more exposed (Table 3) than predicted by the MD simulation at 177 °C, then the computed decay times τ_{comp} for the four tyrosine residues are as follows: 430 ps for Tyr-10, 437 ps for Tyr-12, 148 ps for Tyr-23, and 32 ps for Tyr-115. This results in a simulated decay that can be fitted with a double-exponential with decay times τ_1 = 420 ps and τ_2 = 90 ps and respective pre-exponential coefficients A_1 = 2.4 and A_2 = 1.6 (Figure 7b), close to the experimentally observed decay at 65 °C (τ_1 = 559 ps, τ_2 = 89 ps; A_1 = 2.23, A_2 = 1.77). In fact when we assume that all tyrosine residues are water exposed in the denatured protein, then the analysis of the simulated decay that is generated using the same values of τ_0, ϕ_F, κ^2, n and spectral integral (SI) (as in Table 3) for all four tyrosine residues but with different values of R for Tyr-12 (Supporting Information, Table SI.1) gives the values τ_1 = 420 ps (A_1 = 1.92) and τ_2 = 162 ps (A_1 = 2.08), which are close to those experimentally observed at 80 °C: τ_1 = 510 ps (A_1 = 2.07) and τ_2 = 72 ps (A_1 = 1.93). A number of simulation possibilities and the results of their analysis are

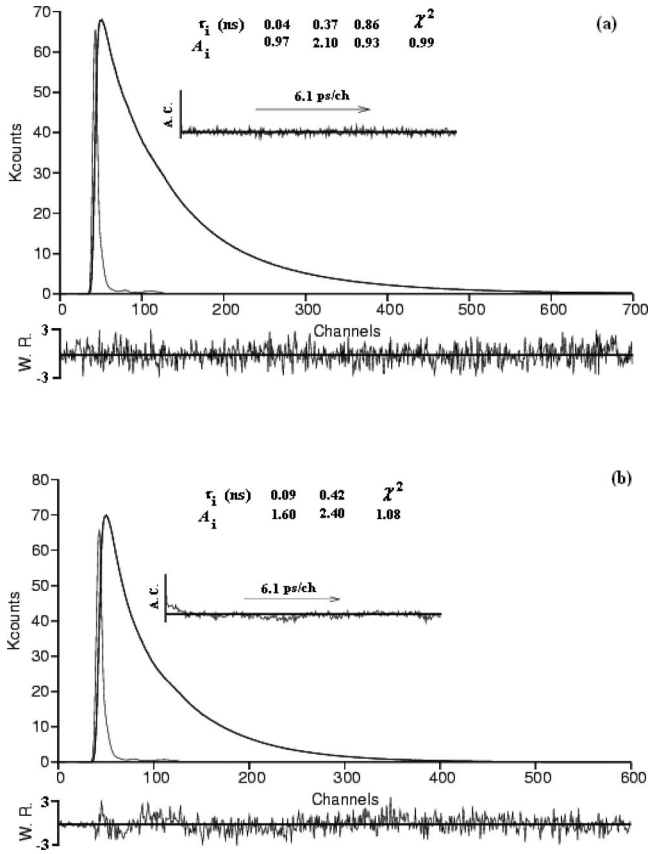

Figure 7. Analysis of a theoretical decay of cytochrome c'' generated using the calculated four decay times presented in (a) Table 2 and (b) Table 3, with noise. (a) The decay can be fitted with a triple-exponential with decay times and pre-exponentials of $\tau_1 = 860$ ps ($A_1 = 0.93$), $\tau_2 = 370$ ps ($A_2 = 2.10$), and $\tau_3 = 40$ ps ($A_3 = 0.97$). (b) The decay is best fitted with a double-exponential with decay times and pre-exponentials of $\tau_1 = 420$ ps ($A_1 = 2.40$) and $\tau_2 = 90$ ps ($A_2 = 1.60$).

presented in Table SI.1 in Supporting Information. These results indicate that for concordance between the experimental and theoretical decays at high temperatures, Tyr-12 must be water exposed at 80 °C; that is, the increase of τ_1 is the combined result of increasing the distance to the heme and the exposition of Tyr-12 to water (unfolding in that region).

Therefore in unfolded Cyt c'', τ_1 now represents Tyr-10 at $R = 20.3$ Å and Tyr-12 at 24.6 Å, and τ_2 represents Tyr-23 at 17.8 Å and Tyr-115 at 11.7 Å. As in the case of the fluorescence decay at 23 °C, the individual fluorescence decay times at 80 °C are experimentally unresolved, such that Tyr-10 and Tyr-12 continue to be described by a single decay time (τ_1) and Tyr-23 and Tyr-115 are predicted by τ_2.

We have previously shown in the case of thermal unfolding of ubiquitin (with a single tyrosine residue) that different individual lifetimes could be assigned to the native and the unfolded state such that these could then be used as a tool to distinguish between the two states. However, for Cyt c'' this is not possible, as is seen in the case of fluorescence decay at 23 °C, which requires two decay times to describe the native state. Also, as the protein unfolds, more decay times and respective pre-exponential coefficients are expected to appear, corresponding to the unfolded state. However, if the decay times in the unfolded state are sufficiently close to those of the native state, then mixing of the decay times occurs and this results not only in the persistence of two decay times over the entire temperature range of unfolding but also the observation of only small changes in the decay times and respective pre-exponential coefficients. Therefore, it is not possible to extract exact thermodynamic information for Cyt c'' from the pre-exponential coefficients, as we were able to do for ubiquitin.[1] Curiously, the pre-exponential coefficients observed experimentally in the case of Cyt c'' show a peculiar trend where no crossing between the two pre-exponential coefficients is observed but the midpoint of A_1 and A_2 occurs approximately at 62.0 °C, close to $T_m = 61.9 \pm 1$ °C from DSC measurements. Therefore, although mixing of decay times of the two states occurs, we can still estimate the T_m from the change in the trend of pre-exponential coefficients.

In conclusion, an increase in τ_1 and A_1 from 55 to 80 °C assigned to the displacement of Tyr-12 from the heme indicates the loss of structure of α-helix I (Thr-3:Asn-20) located in the N-terminal region of the protein whereas the assignment of Tyr-115 to the more quenched decay time τ_2 from 23 to 80 °C, suggests the presence of residual structure of α-helix V (Ser-107:Thr-118) located in the C-terminal region of the protein even at 80 °C. Comparison of structures at 27 and 177 °C shows that at 177 °C, one of the histidine ligands, His95 is completely displaced with no secondary structure in its surrounding region; that is, it is not a source of compactness in the denatured state (Supporting Information, Figure SI. 2).

Conclusions

The results presented here show that an effective and quantitative application of TRFS to probe protein structural changes can be achieved by exploiting the often disregarded information contained in the pre-exponential coefficients of fluorescence decays. For the specific case of heme proteins, the fluorescence decay times are controlled by excited-state energy transfer (FRET), which is directly dependent on the fluorescence lifetime of the individual tyrosine residue in the absence of quenching (τ_0) and inversely dependent on the ratio (R_0/R), where R is the center-to-center distance between the tyrosine ring and Fe^{3+} of the heme and R_0, the characteristic distance at which the efficiency of energy transfer is 50%. As a result of this direct correlation of the experimentally observed decay times (τ_i) to R, changes in structure could be detected in different regions of the protein by coupling the information from the fluorescence decays with MD simulations at different temperatures. The fluorescence decays of oxidized Cyt c'' are double-exponential at 23 °C with decay times $\tau_1 = 430$ ps and $\tau_2 = 90$ ps and respective pre-exponential coefficients $A_1 = 2.08$ and $A_2 = 1.92$, suggesting that two tyrosines could be described with a single decay time of ~430 ps and the other two with a decay time of 90 ps for native folded Cyt c''. From MD simulations of the native structure, the R value of each tyrosine residue was calculated, leading to the assignment of Tyr-10 and Tyr-23 to τ_1 and Tyr-12 and Tyr-115 to τ_2 at 23 °C.

With increasing temperature, changes in the decay times and pre-exponential coefficients were observed, suggesting the need for a new assignment of decay times to tyrosine residues at higher temperatures. Specifically, the increase in τ_1 and A_1 from 55 to 70 °C was attributed to the displacement of Tyr-12 from the heme and exposure to water, which indicates unfolding in this region. Likewise the permanence of $\tau_2 \approx 100$ ps from 20 to 80 °C indicated that Tyr-115 remains close to the heme throughout unfolding. Therefore, according to this analysis, the unfolding of Cyt c'' occurs in two stages: the N-terminal region, comprising α-helix I and Tyr-10 and Tyr-12, appears to melt first, whereas the protein core that comprises the additional four helical structures shows higher stability and remains essentially unchanged up to 80 °C.

Acknowledgment. The work was supported by the Fundação para a Ciência e a Tecnologia (FCT), Portugal, Projects POCI/QUI/56585/04, POCI/BIA-PRO/57263/04 and PPCDT/QUI/58985/2004 and by the European Commission, 5th Framework Programme contract QLK3-CT-2000-00640. M.N. acknowledges a post doctoral grant from FCT, SRFH/BPD/27128/2006. The authors would like to thank the reviewers for their suggestions and careful review of the manuscript.

Supporting Information Available: This material is available free of charge via the Internet at http://pubs.acs.org.

References and Notes

(1) Noronha, M.; Lima, J. C.; Bastos, M.; Santos, H.; Maçanita, A. L. *Biophys. J.* **2004**, *87*, 2609.

(2) Faria, T. Q.; Lima, J. C.; Bastos, M.; Maçanita, A. L.; Santos, H. *J. Biol. Chem.* **2004**, *279*, 48680.

(3) Noronha, M.; Lima, J. C.; Paci, E; Santos, H.; Maçanita, A. L. *Biophys. J.* **2007**, *92*, 4401.

(4) Gryczynski, Z.; Lubkowski, J.; Bucci, E. *Methods Enzymol.* **1997**, *278*, 538.

(5) Brennan, L.; Turner, D. L.; Fareleira, P.; Santos, H. *J. Mol. Biol.* **2001**, *308*, 353.

(6) Enguita, F. J.; Pohl, E.; Turner, D. L.; Santos, H.; Carrondo, M. A. *J. Biol. Inorg. Chem.* **2006**, *11*, 189.

(7) Weber, G.; Teale, F. W. *J. Faraday Soc. Discuss.* **1959**, *27*, 134.

(8) Gryczynski, Z.; Fronticelli, C; Gratton, E.; Lubkowski, J.; Bucci, E. *Biochemsitry III*; SPIE: Bellingham, WA. 1994; Vol. 2137, 129.

(9) Janes, S. M.; Holtom, G.; Ascenzi, P.; Brunori, M.; Hochstrasser, R. M. *Biophys. J.* **1987**, *51*, 653.

(10) Das, T. K.; Mazumdar, S. *Eur. J. Biochem.* **1995**, *227*, 823.

(11) Costa, H. S.; Santos, H.; Turner, D. L.; Xavier, A. V. *Eur. J. Biochem.* **1992**, *208*, 427.

(12) Price, N. J.; Brennan, L.; Faria, T. Q.; Vijgenboom, E.; Canters, G. W.; Turner, D. L.; Santos, H. *Protein Expression Purif.* **2000**, *20*, 444.

(13) Noronha, M.; Lima, J. C.; Lamosa, P.; Santos, H.; Maycock, C.; Ventura, R.; Maçanita, A. L. *J. Phys. Chem. A* **2004**, *108*, 2155.

(14) Striker, G.; Subramaniam, V.; Seidel, C. A. M.; Volkmer, A. J. *J. Phys. Chem. B* **1999**, *103*, 8612.

(15) Brooks, B. R.; Bruccoleri, R. E.; Olafson, B. D.; States, D. J.; Swaminathan, S.; Karplus, M. *J. Comput. Chem.* **1983**, *4*, 187.

(16) MacKerell, A. D., Jr.; Bashford, D.; Bellotand, M.; Dunbrack, R. L., Jr.; Evanseck, J. D.; Field, M. J.; Fischer, S.; Gao, J.; Guo, H.; Ha, S.; Joseph-McCarthy, D.; Kuchnir, L.; Kuczera, K.; Lau, F. T. K.; Mattos, C.; Michnick, S.; Ngo, T.; Nguyen, D. T.; Prodhom, B.; Reiher, W. E.; Roux, B.; Schlenkrich, B.; Smith, J. C.; Stote, R. H.; Straub, J.; Wiórkiewicz-Kuczera, J.; Yin, D.; Karplus, M. *J. Phys. Chem. B* **1998**, *102*, 3586.

(17) Im, W.; Lee, M. S.; Brooks, C. L. *J. Comput. Chem.* **2003**, *24*, 1691.

(18) Valeur, B. *Molecular Fluorescence: Principles and Applications*; Wiley-VCH Verlag GmbH: Germany, 2002; p 72.

(19) Gryczynski, Z.; Bucci, E.; Kusba, J. *Photochem. Photobiol.* **1993**, *58*, 492.

JP805781R